Open Chem., 2018; 16: 50–63 DE GRUYTER

Research Article Open Access

Lamya H. Al-Wahaibi, Munusamy Govindarajan, Ali A. El-Emam, Mohamed I. Attia*

Spectroscopic (FT-IR, FT-Raman, UV, ¹H and ¹³C NMR) insights, electronic profiling and DFT computations on ({(*E*)-[3-(1*H*-imidazol-1-yl)-1-phenylpropylidene] amino}oxy)(4-nitrophenyl)methanone, an imidazole-bearing anti-*Candida* agent

https://doi.org/10.1515/chem-2018-0005 received October 25, 2017; accepted December 2, 2017.

გ

Abstract: The anti-*Candida* agent, ({(E)-[3-(1H-imidazol-1-yl)-1-phenylpropylidene]amnio}oxy(4-nitropheny) methanone (IPAONM), was subjected to comprehensive spectroscopic (FT-IR, FT-Raman, UV–Vis ¹H and ¹³C NMR) characterization as well as Hartree Fock and density functional theory computation studies. The selected optimized geometric bond lengths and bond angles of the IPAONM molecule were compared with the experimental values. The calculated wavenumbers have been scaled and compared with the experimental spectra. Mulliken charges and natural bond orbital analysis of the title molecule were calculated and interpreted. The energy and oscillator strengths of the IPAONM molecule were calculated by time-dependent density functional theory (TD-DFT). In addition, frontier molecular orbitals and molecular

electrostatic potential diagram of the title compound were computed and analyzed. A study on the electronic properties, such as HOMO, HOMO-1, LUMO and LUMO+1 energies was carried out using TD-DFT approach. The ¹H and ¹³C NMR chemical shift values of the title compound were calculated by the gauge independent atomic orbital method and compared with the experimental results.

Keywords: Imidazole, FT-IR, FT-Raman, HF, DFT, Anti-*Candida*.

1 Introduction

Invasive fungal infections are an ever-growing health problem worldwide causing high rates of morbidity and mortality particularly in chronically ill individuals or those taking anticancer or immunosuppressant drugs [1]. *Candida albicans* (*C. albicans*) has been identified as a leading invasive fungal pathogen and accounts for up to 70% of global fungal incidents with 30-55% mortality rate [2]. The current repertoire of antifungal drugs to treat *C. albicans* is limited and suffers from significant adverse effects and resistance [3,4]. Consequently, it is highly desirable to search for new alternative anti-*C. albicans* agents endowed with high potency and improved safety.

Azole antifungal agents are widely used to treat invasive fungal infections caused by $\it C.~albicans$ and they rapidly became the most clinically prescribed antifungals worldwide [5]. They target sterol 14 α -demethylase enzyme leading to fungal cell death due to inhibition of the biosynthesis of ergosterol, a vital component of the fungal cell membrane, and accumulation of the methylated sterol side products [6,7].

Lamya H. Al-Wahaibi: Department of Chemistry, College of Sciences, Princess Nourah Bint Abdulrahman University, Riyadh 11671, Saudi Arabia

Munusamy Govindarajan: Department of Physics, Avvaiyar Government College for Women (AGCW), Karaikal, Puducherry 609602, India; Department of Physics, Arignar Anna Government Arts and Science College for Women (AAGASC), Karaikal, Puducherry 609602, India

Ali A. El-Emam: Department of Pharmaceutical Chemistry, College of Pharmacy, King Saud University, P.O. Box 2457, Riyadh 11451, Saudi Arabia; Department of Medicinal Chemistry, Faculty of Pharmacy, University of Mansoura, Mansoura 35516, Egypt

^{*}Corresponding author: Mohamed I. Attia: Department of Pharmaceutical Chemistry, College of Pharmacy, King Saud University, P.O. Box 2457, Riyadh 11451, Saudi Arabia; Medicinal and Pharmaceutical Chemistry Department, Pharmaceutical and Drug Industries Research Division, National Research Centre (ID: 60014618), El Bohooth Street, Dokki, Giza 12622, Egypt, E-mail: mattia@ksu.edu.sa

The title compound, namely $(\{(E), [3, (1H-imidazol-$ 1-yl)-1-phenylpropylidenel amnio\oxy(4-nitropheny) methanone (IPAONM) is an imidazole-bearing anti-C. albicans agent with minimum inhibitory concentration (MIC) value of 0.7 µmol/mL being about fourfold more potent than the reference antifungal drug, fluconazole [8]. The displayed anti-C. albicans activity of the IPAONM molecule represents a strong motive for exploring a comprehensive spectroscopic characterization density functional theory (DFT) computations on this interesting compound. Thus, its Mulliken charges, natural bond orbital (NBO) analysis and molecular electrostatic potential (MEP) were investigated. NBO analysis determines the possible intermolecular delocalization or hyper-conjugation for the IPAONM molecule. Moreover, its frontier molecular orbitals (FMO), HOMO and LUMO energies were also computed. The HOMO and LUMO molecular orbitals investigations give insight into the possible way in which the IPAONM molecule can interact with its target receptors. The results of the current study could provide a useful platform to develop new chemical entities characterized by potent and safe anti-C. albicans profile.

2 Experimental Section

2.1 General

The FT-IR spectrum of the IPAONM molecule has been recorded with a Perkin-Elmer 180 Spectrometer in the range of 4000-400 cm⁻¹ with spectral resolution ± 2 cm⁻¹. Its FT-Raman spectrum was also recorded in the same instrument with FRA 106 Raman module equipped with Nd: YAG laser source operating in the region 100-4000 cm⁻¹ at 1.064 µm line widths with 200 mW powers. The spectra were recorded with scanning speed of 30 cm⁻¹. min⁻¹ with spectral width of 2 cm⁻¹. The frequencies of all sharp bands were accurate to ± 1 cm⁻¹. NMR spectra of the IPAONM were recorded on a Bruker NMR spectrometer (Bruker Biospin, Billerica, MA, USA). ¹H spectrum was run at 500 MHz and ¹³C spectrum was run at 125 MHz in deuterated dimethyl sulfoxide (DMSO-d6). The UV-Vis spectrum of the title molecule was registered in the range of 200-400 nm in acetonitrile using Shimadzu UV-2101 PC, UV-Vis recording spectrometer. All solvents and reagents were purchased from Sigma-Aldrich Chemie GmbH (Taufkirchen, Germany) and were pure enough to be used without further purification.

2.2 Synthesis

Preparation of $(\{(E)-[3-(1H-imidazol-1-yl)-1-phenylpropylidene])$ aminooxy)(4-nitro phenyl)methanone (5)

The title compound 5 was prepared according to the previously reported method [8]. The NMR spectral data of compound 5 are in agreement with the previously reported ones [8].

2.3 Quantum Chemical Calculations

The entire quantum chemical calculations have been performed using Hartree Fock (HF) and density functional theory (DFT, B3LYP) methods with 6-311G(d,p) basis set using the Gaussian 09 W program [9]. The optimized structural parameters have been evaluated for the calculations of vibrational frequencies at different level of theories. At the optimized geometry for the IPAONM molecule no imaginary wavenumbers were obtained, so there is a true minimum on the potential energy surface. As a result, the calculated frequencies, reduced masses, force constants, infrared intensities, Raman activities and depolarization ratios were obtained. In order to improve the computed values to be in agreement with the observed experimental values, it was necessary to scale down the calculated harmonic frequencies. Hence, the wavenumbers calculated at HF level were scaled by 0.9067 and the range of wavenumbers above 1700 cm⁻¹ were scaled by 0.958 and below 1700 cm⁻¹ by 0.983 for the B3LYP method [10,11]. The assignments of the calculated modes have been made on the basis of the corresponding PEDs. The vibrational frequencies were calculated using VEDA program [12]. GaussView program [13] was used in order to get visual animation and also for the verification of the normal modes assignments. The electronic absorption spectra for the optimized molecule were calculated with the time dependent density functional theory (TD-DFT) at B3LYP/6-311G(d,p) level.

Ethical approval: The conducted research is not related to either human or animals use.

3 Results and Discussion

3.1 Synthesis

The title compound 5 was prepared by adopting the previously reported literature procedure [8] as illustrated in Scheme S1. The spectral data of the title compound 5 are consistent with the previously reported ones [8].

3.2 Molecular Geometry

Molecules bearing oxygen or nitrogen substituents on their ring systems have the mono substituent co-planar with the ring. The selected optimized DFT geometries of the IPAONM molecule are calculated by HF and B3LYP methods with 6-311G(d,p) as a basic set with atom numbering as shown in Figure 1. The calculations are converged to optimized geometries, which correspond to the true energy minima, as revealed by the lack of imaginary frequencies in the vibrational mode calculations.

3.3 Geometric Structure

A conformation analysis was carried out on the IPAONM molecule in order to determine its most stable conformation. The crystal structure of the title compound is indicated in the Figure 2. The potential energy obtained by the rotation of the two dihedral angles C5-C7-C8-C9 and O16-C17-C18-O19 group from 0° to 360° in PM6 method is depicted in Figure 3. The most stable conformers are at 90° for SC1 and at 320° for SC2 with energy value = 0.0761424 a.u. The optimized geometry of the title molecule afforded one conformer at this stage. The selected optimized parameters were collected and compared with the experimental X-ray data [8] as illustrated in Table 1. The most stable conformer possesses the global minima on its potential energy surface as its calculated vibrational spectrum contains no imaginary wavenumbers.

These optimized parameters are in agreement with the crystallographic values (Table 1). The aromatic N-O bond distances of IPAONM were found to have lower values in case of HF calculations with respect to B3LYP computations. The oxygen—carbon bonds are not of the same length. The elongation of O16-C17 could be attributed to its presence in the main chain. The N-C bond distances are present between 1.469 to 1.265 Å. The N42-C22 is the longest bond among the N-C bonds and its length is 1.469 Å. In the imidazole ring, the bonds N10-C9, N13-C12, N13-C14, N10-C11 and N10-C14 are 1.453, 1.355, 1.371, 1.309 and 1.414 Å in length, respectively.

The HF and B3LYP calculations also gave dihedral angles values that are consistent with the selected experimental values (Table 1). The highest value was 127.82° in case of C9-N10-C11, while the bond angle C14-N10-C11 possesses the smallest selected bond angle being about 104.9°. Moreover, the bond angles, O19-C17-O16 and O25-N42-O43 have the values of 125.13° and 123.17°, respectively.

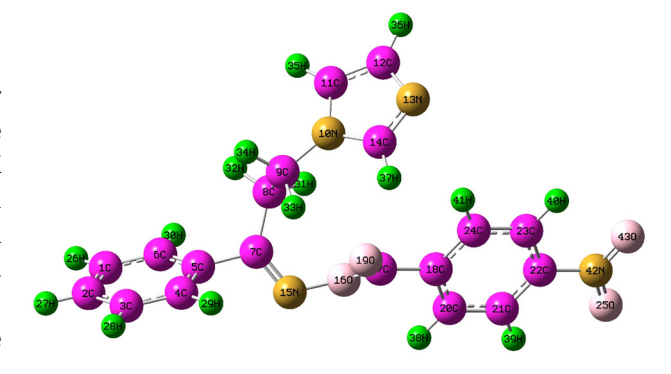


Figure 1: The optimized possible geometric structure with atoms numbering of the IPAONM molecule.

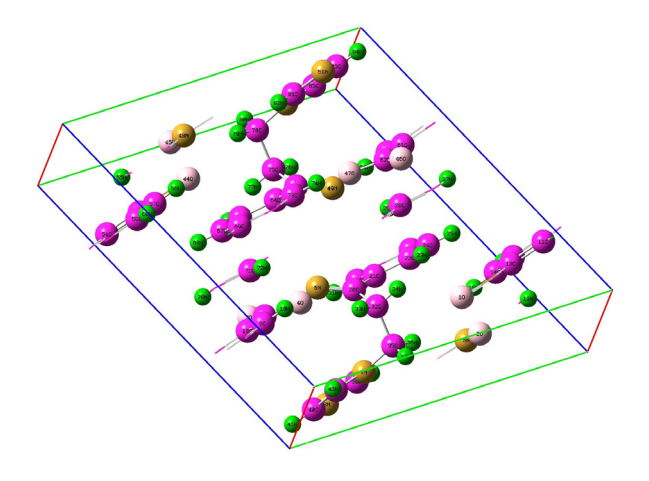


Figure 2: The crystal structure of the IPAONM molecule.

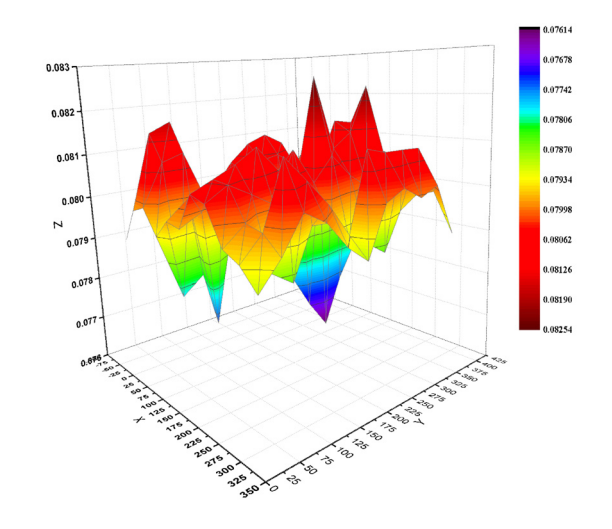


Figure 3: The potential energy scan picture the IPAONM molecule.

Table 1: Selected optimized geometrical parameters and XRD values of bond lengths (Å) and bond angles (°) of the IPAONM molecule.

Parameters	HF/6-	B3LYP/6-	XRD
r drameters	311G(d,p)	311G(d,p)	values
Bond lengths (Å)		,	
N42-043	1.192	1.222	1.219
N42-025	1.195	1.222	1.212
019-C17	1.180	1.196	1.190
O16-N15	1.388	1.418	1.442
016-C17	1.339	1.376	1.347
N42-C22	1.462	1.484	1.469
N15-C7	1.265	1.285	1.278
N10-C9	1.445	1.455	1.453
N13-C12	1.369	1.369	1.355
N13-C14	1.290	1.370	1.371
N10-C11	1.350	1.311	1.309
N10-C14	1.378	1.375	1.414
Bond angles (°)			
N15-O16-C17	114.00	112.71	112.12
025-N42-043	117.52	125.16	123.17
O25-N42-C22	117.93	117.39	117.86
043-N42-C22	117.55	117.45	118.98
016-N15-C7	111.88	111.34	110.00
C9-N10-C14	126.74	126.51	126.51
C9-N10-C11	127.21	127.19	127.82
C14-N10-C11	105.94	105.16	105.49
C14-N13-C12	105.14	105.66	104.9 0
N42-C22-C21	118.71	118.83	119.16
N42-C22-C23	118.76	118.85	118.10
019-C17-016	124.96	124.83	125.13
019-C17-C18	123.63	124.62	124.25
016-C17-C18	111.39	110.54	110.60
N15-C7-C5	115.10	115.52	113.74
N15-C7-C8	125.51	123.76	126.14
N10-C9-C8	112.02	112.35	112.42
N10-C14-N13	112.83	112.35	112.12
N13-C12-C11	110.33	110.58	108.60
N10-C11-C12	105.76	105.66	108.90

3.4 Mulliken Atomic Charges

Mulliken atomic charge calculations have a substantial role in the quantum chemical calculations of molecular systems because they affect a lot of their properties. The calculated Mulliken charge values of the title compound IPAONM are listed in Table S1 and its charge distribution

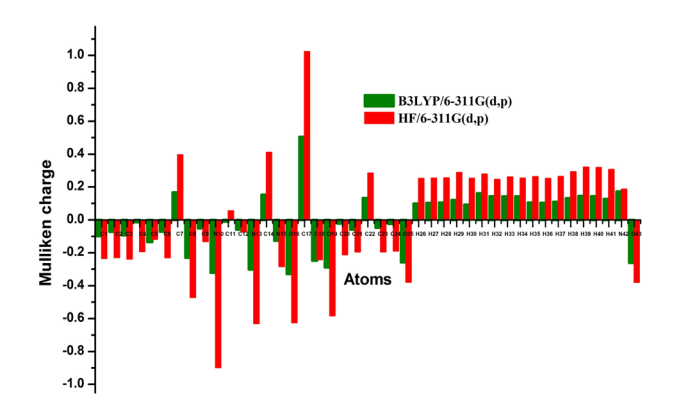


Figure 4: The Mulliken charge distribution for the IPAONM molecule.

is shown in Figure 4. The Mulliken charges of the IPAONM molecule presumably occur due to polarization on the molecule. The charges of the NO, moiety are -0.258427 e on one oxygen atom, -0.259955 e on the other oxygen atom and 0.173708 e⁻ on the nitrogen atom using B3LYP/6-311G(d,p) method which are less than the values obtained by HF/6-311G(d,p) method. All nitrogen atoms are negatively charged except for N42. The Mulliken charges on nitrogen atoms N10 and N13 are more negative than that on N15. All aromatic carbon atoms are negatively charged using B3LP/6-311G(d,p) method except C22 due to its bonding with the nitro group. C7 and C17 are the highest positively charged carbon atoms by B3LYP method due to their bonding to nitrogen and oxygen atoms, respectively. All hydrogen atoms are positively charged using both HF and B3LP methods (Figure 4).

3.5 Frontier Molecular Orbitals (FMOs)

HOMO is the highest occupied molecular orbital and LUMO is the lowest-lying unoccupied molecular orbital and together they are named frontier molecular orbitals (FMOs). The FMOs play a crucial role in many optical and electric properties as well as in quantum chemistry and UV-Vis spectra of molecules [14]. The HOMO makes up the ability to donate electrons, while LUMO as an electron acceptor. The energy gap between HOMO and LUMO decides the kinetic stability, chemical reactivity, optical polarizability and chemical hardness-softness of a molecule [15].

The energies of the four important molecular orbitals, the highest and the second highest occupied MO's (HOMO and HOMO-1) as well as the lowest and the second lowest unoccupied MO's (LUMO and LUMO+1), of the IPAONM molecule were calculated using B3LYP method

Table 2: Calculated molecular orbital energy values of the title molecule.

TD-DFT/B3LYP/	Gas	Chloroform
6-311G(d,p)	Phase	Phase
E _{total} (Hartree)	-1253.72	-1253.42
E _{HOMO} (eV)	-6.56868	-6.27965
E _{LUMO} (eV)	-3.11963	-2.86721
ΔE _{HOMO-LUMO gap} (eV)	-3.44905	-3.41245
E _{HOMO-1} (eV)	-7.14673	-6.7403
E _{LUMO+1} (eV)	-2.09123	-1.68318
$\Delta E_{\text{HOMO-1-LUMO+1 gap}}$ (eV)	-5.0555	-5.05713
Electronegativity χ (eV)	4.8441	4.5734
Chemical hardness η (eV)	1.7245	1.7062
Electrophilicity index ψ (eV)	6.8036	6.1293
Dipole moment (Debye)	7.3089	8.4214

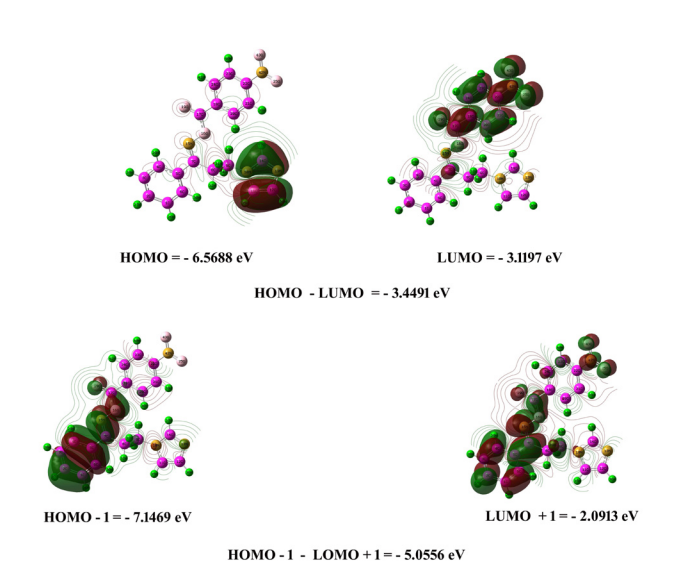


Figure 5: The molecular orbitals and energies for the HOMO-1, HOMO, and LUMO and LUMO+1 of the IPAONM molecule.

at 6-311G(d,p) level. The 3D plots of the HOMO-1, HOMO, LUMO and LUMO+1 orbitals computed at the B3LYP/6-311G(d,p) level for the IPAONM molecule are illustrated in Figure 5. The positive phase is red and the negative one is green. It is clear from Figure 5 that while the HOMO is localized on the imidazole moiety of the IPAONM molecule, the LUMO is localized on the nitrophenyl ring. However, the HOMO-1 is localized on the other phenyl ring, LUMO+1 is localized on both phenyl ring and the nitro group of the title molecule. Both the HOMOs and the LUMOs are mostly π -antibonding type orbitals.

The calculated energy values of the title molecule are HOMO = -6.5688 and LUMO = -3.1197 eV. The value of energy separation between the HOMO and LUMO is -3.4491 eV (Table 2). The HOMO–LUMO energy gap of the title molecule explains the charge transfer interaction inside the molecule, which influences its bioactivity. Increasing

the value of the energy gap indicates more stability of the molecule.

3.6 Electrostatic Potential, Total Electron Density and Molecular Electrostatic Potential

The electrostatic potential (ESP), total electron density (TED) and molecular electrostatic potential (MEP) of the title molecule are illustrated in Figure 6. The yellowish blob in the ESP Figure reflects the negative portion of the title molecule. However, the MEP diagram represents the constant electron density surface of the IPAONM molecule. The MEP diagram is a useful tool to analyze the reactivity of the molecules toward electrophiles and nucleophiles. In the majority of the MEPs, the maximum positive and negative regions in the molecule are indicated by red and green colors which are the preferred sites to be attacked by electrophiles and nucleophiles, respectively. The importance of the MEPs resides in the fact that they display at the same time the molecular size, shape as well as positive, negative and neutral electrostatic potential regions of the molecule in terms of color grading. They are also a very useful tool correlating molecular structure with the physiochemical properties of the molecule [16-18].

The electrostatic potential at the surface of the IPAONM molecule is represented by different colors in the order red < orange < yellow < green < blue in the range between -0.0568 a.u. (deepest red) to 0.0568 (deepest blue). The blue color indicates the strongest attraction, while the red color indicates the strongest repulsion. The negative potential was manifested over the electronegative oxygen atoms of the nitro group in the MEP diagram of the title molecule with values of -0.04086 and -0.04019 a.u.

3.7 Natural Bond Orbital (NBO) Analysis

The larger the stabilization energy value of the molecule, the more significant is the interaction between the donors and acceptors, i.e. the more giving tendency there is from donors to acceptors, the greater the extent of conjugation of the entire system. The intramolecular interactions of the title molecule are formed by the orbital overlap between $\sigma(\text{C-N})$, $\sigma^*(\text{C-N})$, $\sigma(\text{N-C})$, $\sigma^*(\text{N-C})$, $\sigma(\text{C-O})$, $\sigma^*(\text{C-O})$, $\sigma^*(\text{C-N})$, $\sigma^*(\text{C-N})$, $\sigma^*(\text{N-O})$ and $\sigma^*(\text{C-C})$, $\sigma^*(\text{C-C})$ bond orbitals. These fundamental interactions were observed as a gain in the electron density (ED) in the C-C antibonding orbitals that weaken the respective bonds. These intramolecular charge transfers $(\sigma \to \sigma^*, \ \pi \to \pi^*)$ can induce large nonlinearity of the IPAONM molecule.

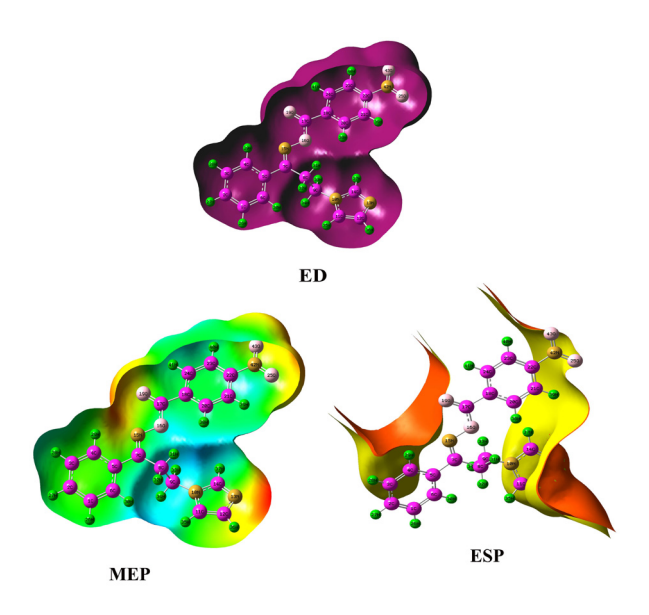


Figure 6: Electrostatic potential (ESP), electron density (ED) and the molecular electrostatic potential map (MEP) for the IPAONM molecule.

Natural bond orbital (NBO) analysis has been carried out on the IPAONM molecule at the B3LYP/6-311G(d,p) level in order to elucidate its possible intramolecular, rehybridization and delocalization of the electron density within the molecule. The intramolecular hyperconjugation interactions of the σ and π electrons of C-N, N-C, C-O, O-N and N-O to the anti C-C, C-H, C-N and N-O bonds in the title molecule lead to stabilization of the respective moieties within the molecule as evident from Table S2. The strong hyperconjugative interactions of the σ electron of σ (N10– C11) are distributed to σ^* (C9-N10), N10-C14, C11-C12, C12-N13, C12-H36, N13-C14 and C14-H37 of the imidazole ring with energy values of 1.86, 2.47, 1.47, 0.73, 3.19, 0.63 and 2.89 kcal/mol, respectively. On the other hand, the σ (C17-O19) and π (C17-O19) bonds are distributed to π^* (C18-C20) with energy values of 1.08 and 4.36 kcal/mol, respectively. In addition, in the LP N10 and LP N13 are distributed to the LP*(1) (C11-C12) bond with energy values of 30.68 and 5.46 kcal/mol, respectively.

3.8 Electronic Absorption Spectra

Based on a fully optimized ground-state structure of the of the IPAONM molecule, B3LYP/6-311G(d,p) calculations have been carried out to determine its low-lying excited states. The experimental (in acetonitrile) and theoretical UV absorption wavelengths (in acetonitrile, aniline, chloroform, DMSO, ethanol, methanol and toluene) of

Table 3: The calculated absorption wavelengths (λ), excitation energies (E) and oscillator strengths (f) of the IPAONM molecule using B3LYP/311G(d,p) level.

Solvent	λ (nm)	E (ev)	f (a.u.)	Major contribution
Acetonitrile	411.65	3.01	0.0007	HOMO->LUMO (100%)
	358.21	3.46	0.1343	H-1->LUMO (99%)
	318.02	3.89	0.0001	H-9->LUMO (86%)
	315.99	3.92	0.0029	H-2->LUMO (99%)
	299.80	4.13	0.0023	H-3->LUMO (86%),
Aniline	409.14	3.03	0.0008	HOMO->LUMO (100%)
	355.99	3.48	0.1473	H-1->LUMO (99%)
	319.94	3.87	0.0000	H-9->LUMO (85%)
	313.55	3.95	0.0037	H-2->LUMO (99%)
	299.59	4.14	0.0040	HOMO->L+1 (87%)
Chloroform	408.05	3.03	0.0007	HOMO->LUMO (100%)
	354.22	3.50	0.1419	H-1->LUMO (99%)
	320.89	3.86	0.0000	H-9->LUMO (84%)
	312.13	3.97	0.0036	H-2->LUMO (99%)
	299.97	4.13	0.0035	HOMO->L+1 (96%)
DMSO	411.85	3.01	0.0007	HOMO->LUMO (100%)
	358.53	3.45	0.1382	H-1->LUMO (99%)
	317.93	3.89	0.0001	H-9->LUMO (86%)
	316.13	3.92	0.0030	H-2->LUMO (99%)
	299.86	4.13	0.0023	H-3->LUMO (88%)
Ethanol	411.34	3.01	0.0007	HOMO->LUMO (100%)
	357.98	3.46	0.1353	H-1->LUMO (99%)
	318.24	3.89	0.0001	H-9->LUMO (86%)
	315.73	3.92	0.003	H-2->LUMO (99%)
	299.71	4.13	0.0025	H-3->LUMO (83%)
Methanol	411.59	3.01	0.0007	HOMO->LUMO (100%)
	358.12	3.46	0.1334	H-1->LUMO (99%)
	318.06	3.89	0.0001	H-9->LUMO (86%)
	315.93	3.92	0.0029	H-2->LUMO (99%)
	299.78	4.13	0.0023	H-3->LUMO (86%)
Toluene	405.66	3.05	0.0007	HOMO->LUMO (100%)
	349.72	3.54	0.1486	H-1->LUMO (99%)
	323.52	3.83	0.0000	H-9->LUMO (78%)
	307.91	4.02	0.0041	H-2->LUMO (98%)
	301.72	4.10	0.0033	HOMO->L+1 (99%)

the title compound are shown in Figure S1 and Table 3. Calculations involving the vertical excitation energies, oscillator strengths (f) and wavelengths (λ) have been performed and the results were compared with experimental values [19]. The major contributions of the transitions of the IPAONM molecule were designated with the aid of SWizard program [20]. The predicted wavelengths using B3LYP/6-311G(d,p) calculations in acetonitrile are 411.65, 358.21, 318.02, 315.99 and 299.80 nm, whereas the experimental wavelengths in acetonitrile are 235.10 and 282.80 nm. In view of the calculated absorption spectra of the title compound, the maximum absorption wavelengths correspond to the electronic transitions

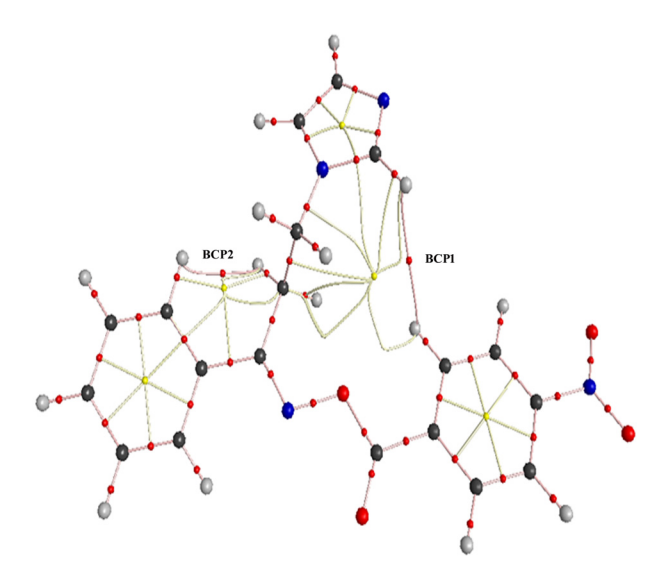
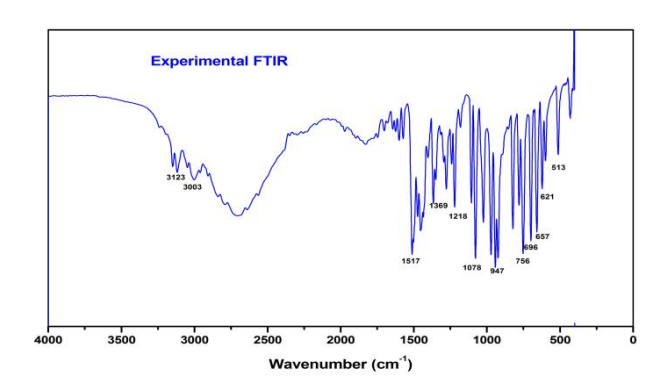


Figure 7: The topological diagram of the IPAONM molecule.

from the highest occupied molecular orbital HOMO to the lowest unoccupied molecular orbital LUMO with 100% contribution and the transitions from HOMO-9 to LUMO with 85% except with chloroform and toluene.

3.9 Topological Analysis

The structure of the IPAONM molecule was also analysed by Bader's charge electron density topological analysis [21,22]. In the topological atoms in molecules (AIM) theory, the chemical bonds and molecular reactivity are interpreted in terms of the total molecular electronic density $\rho(r)$ and its corresponding Laplacian $\nabla^2 \rho(r)$. The $\rho(r)$ and $\nabla^2 \rho(r)$ values at the bond critical points (BCP1 and BCP2) allow the characterization of the chemical bonds between atoms of the molecule. Different studies have pointed out that formation of hydrogen bonds was associated with the appearance of BCP1 and BCP2 between hydrogen atoms and the acceptor atoms, which are linked by the concomitant bond path [23-25]. The positive Laplacian value of the electron density $\nabla^2 \rho(\mathbf{r})$ indicates that the interaction is dominated by the contraction of charge away from the interatomic surface toward each nuclei. Figure 7 illustrated the AIM molecular graphic of the title molecule showing its different bonds and ring critical points obtained by B3LYP/6-311G(d,p) method. The Laplacian values of the IPAONM molecule at the BCP1 and BCP2 of H37-H38 and H30-H32 bonds are 0.0069 and 0.0473 a.u., respectively, while their Lagrangian kinetic energy density G(r) and energy density H(r) values are 0.0013, 0.0096 and 0.0004, 0.0022 a.u., respectively.



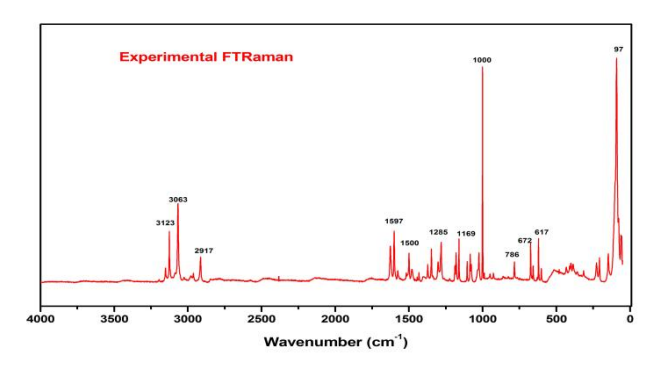


Figure 8: Experimental FT-IR and FT-Raman and spectra of the IPAONM molecule.

3.10 Vibrational Analysis

All vibrations are active in both Raman and infrared absorptions. The detailed vibrational assignments of the experimental wavenumbers are based on normal mode analyses and a comparison with theoretically scaled wavenumbers with PED by B3LYP method. Since the scaled wavenumbers following B3LYP/6-311G(d,p) method were found to be close to the experimental data than the results obtained using HF method, so only the PEDs from this set of data are discussed in detail. The observed and simulated FT-IR and laser Raman spectra of the IPAONM molecule are shown in Figures 8 and 9, respectively. The observed and scaled theoretical frequencies using HF and DFT (B3LYP) with 6-311G(d,p) basis set, infrared intensities and Raman activities of B3LYP/6-311G(d,p) are listed in Table 4.

3.10.1 C-H Vibrations

Aromatic derivatives gave rise to C-H stretching, C-H inplane and C-H out-of-plane bending vibrations. Aromatic compounds commonly exhibit multiple weak bands in the region of 3100–3000 cm⁻¹ due to aromatic C-H stretching vibrations and they are not appreciably affected by the

 Table 4: Detailed assignments of vibrational bands of the IPAONM molecule along with potential total energy distribution.

No.	Experime	ntal	Theoretical					Vibrational
			HF/6-311G(d,p)	B3LYP/6-311G(D,P)				Assessment
	FT-IR	FT-Raman		<u> </u>	<u>S</u>	Unscaled	Scaled	
1	3123		3163	2.77	109.37	3263	3126	γСН
2			3137	4.33	120.85	3236	3100	γСН
3			3131	2.71	86.53	3230	3094	γСН
4			3121	2.44	133.25	3229	3093	γСН
5			3119	1.66	57.36	3228	3092	γСН
6			3107	1.85	63.82	3216	3081	γСН
7			3089	3.20	79.48	3210	3076	γСН
8			3085	1.61	42.21	3208	3073	γСН
9		3069	3077	14.65	242.65	3196	3062	γСН
10	3052		3067	27.07	114.83	3187	3053	γСН
11			3056	5.34	157.26	3177	3044	γСН
12		3034	3046	0.62	46.73	3168	3035	γСН
13	3003		3037	14.26	3.19	3130	2998	γСН
14		2979	3006	1.01	52.95	3109	2978	γСН
15		2958	2989	12.12	44.49	3083	2953	γСН
16	2925		2952	17.13	112.74	3057	2929	γСН
17	1751		1780	59.55	175.49	1830	1754	γΝΟ
18	1636		1674	26.97	288.61	1667	1639	γCO
19		1627	1618	94.48	22.58	1655	1627	γCC
20	1615		1609	6.54	7.81	1642	1614	γCN
21	1608		1598	4.45	1250.85	1640	1612	γCN
22		1597	1583	13.57	169.37	1614	1586	γCN
23	1575	1577	1517	40.52	6.12	1601	1574	γCN
24	1517	2577	1517	23.02	3.84	1539	1513	γCC
25			1515	3.23	70.83	1530	1504	γCC
26		1500	1502	32.35	6.74	1527	1501	γCN
27	1495	1500	1502	1.89	7.77	1520	1494	γCC
28	1480	1482	1469	9.28	3.09	1506	1481	γCC
29	1400	1402	1466	49.51	14.58	1492	1466	γCC
30	1452		1423	5.53	27.80	1476	1450	γCC
31	1405		1385	15.15	15.27	1476	1411	үСС үСС
				6.68	12.22			
32	1392	13/0	1376			1415	1391	γCC
33	1260	1369	1368	29.56	19.73	1395	1372	γCC
34	1369	4055	1341	0.37	38.20	1386	1362	γCC
35	4220	1355	1334	92.32	356.74	1381	1358	γCC
36	1339		1328	43.02	86.44	1364	1340	γCN
37			1302	20.85	0.30	1358	1335	γCC
38			1288	40.24	73.07	1349	1326	үСС
39	1304	1305	1287	0.46	10.47	1328	1306	үСС
40			1260	0.49	1.15	1319	1297	үСС
41			1244	17.60	21.20	1308	1286	үСС
42		1285	1231	57.22	29.49	1305	1283	γCO
43			1227	19.39	23.72	1290	1268	βСН
44	1240		1220	86.91	11.57	1259	1238	βΟΝΟ
45	1218		1214	494.67	281.68	1248	1227	βΟCΟ
46	1182		1205	8.31	13.79	1211	1190	βСН

Continued Table 4: Detailed assignments of vibrational bands of the IPAONM molecule along with potential total energy distribution.

No.	Experime	ntal	Theoretical			,	Vibrational	
	ET ID	FT Dames	HF/6-311G(d,p)	B3LYP/6-311G(D,P)				Assessment
47	FT-IR	FT-Raman	1107		S	Unscaled	Scaled	0.011
47 48		1169	1196	28.12	13.39	1194	1173	βСН βССС
		1169	1164	0.02	15.05	1187	1167	•
49			1137	0.41	124.18	1181	1161	βСН
50	1107		1111	12.01	9.97	1140	1121	βССС
51	1104		1110	2.85	4.22	1127	1108	βССС
52			1100	26.84	121.88	1118	1099	βСН
53	4070		1097	3.65	2.32	1114	1095	βСН
54	1078		1094	36.51	15.45	1098	1079	βССС
55			1091	37.74	15.26	1091	1073	βССС
56			1085	49.26	13.58	1066	1048	βСН
57		1031	1085	0.28	29.11	1051	1033	βCN
58	1025		1065	16.21	10.97	1042	1025	βССС
59			1056	45.33	2.52	1031	1013	вссс
60			1034	2.92	17.23	1023	1005	βCCN
61			1032	82.61	70.23	1020	1003	βССО
62		1000	1026	0.09	2.20	1017	1000	βСН
63			1016	2.25	17.82	1017	1000	βСН
54			1001	44.72	17.16	1015	998	βCN
65			1001	1.12	0.80	1003	985	βСН
66	973		992	0.70	0.15	993	976	βСН
67	929		980	49.10	3.49	945	929	βCN
68	925	926	971	84.86	8.93	942	926	βCN
59			963	12.78	2.52	918	902	βСО
70			928	37.82	5.46	898	883	βСН
71			920	02.21	48.19	895	880	вссс
72			914	8.79	1.00	871	856	βСН
73			909	55.95	5.04	870	855	βСН
74			899	0.81	0.78	863	849	βСН
75			881	0.53	1.35	859	844	βСН
76			825	9.91	3.84	823	809	βON
77			822	24.08	0.71	817	803	βCN
78	778	786	819	17.45	1.01	789	776	вссс
79			801	4.32	4.59	788	774	βССС
30	758		782	21.70	1.54	780	767	вссс
81			767	8.77	1.69	740	728	βСН
32			728	92.97	0.61	724	712	βCN
33			720	0.07	0.70	723	711	βNO
34			716	4.76	2.46	718	706	φСН
35	696		696	31.13	0.81	708	696	φCCC
36		672	677	2.64	0.27	680	669	φCCO
37	657		670	15.45	0.15	677	666	φCNC
88		645	663	10.91	5.50	654	643	φNCN
89		- 13	655	5.13	1.81	647	636	φСН
90			647	1.95	9.49	642	631	φСН
91	621		640	1.75	4.41	635	624	φСН
92	021	617	626	6.57	8.07	624	613	φCNC

rentiquea Table 4: Detailed assignments of vibrational bands of the IPAONM molecule along with potential total energy distribution.

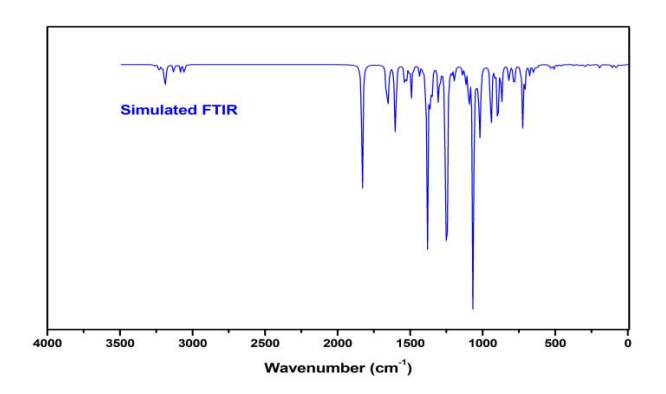
No.	Experime	ntal	Theoretical					Vibrational
			HF/6-311G(d,p) B3LYP/6-311G(D,P)					Assessment
	FT-IR	FT-Raman		1	S	Unscaled	Scaled	
93			530	1.74	1.91	545	536	φСН
94	513		519	8.51	1.99	529	520	φСН
95			491	7.87	3.02	510	501	φСН
96			483	2.21	1.86	485	477	φСН
97			467	0.60	0.33	471	463	φCNC
98		441	448	3.05	0.45	457	449	φСН
99			447	0.03	0.08	421	414	φCON
100		406	424	0.13	1.16	413	406	φСН
101			365	2.01	2.39	371	364	φCCC
102			342	0.61	0.35	342	336	φСН
103			331	0.61	1.92	328	323	φСН
104		319	307	1.49	0.99	326	320	φΝΟC
105			300	1.76	1.23	303	298	φСН
106			286	3.09	2.31	294	289	φСН
107			265	1.10	1.77	259	254	φСН
108		232	233	0.68	1.43	245	241	φCON
109		195	195	5.04	0.72	196	193	φCCC
110			175	1.59	3.08	187	184	φСН
111		146	151	0.67	3.52	141	139	φCCN
112			114	5.17	1.68	110	108	φCCO
113		97	93	0.70	1.64	94	92	φΟCΟ
114			85	3.45	0.46	83	81	φCCC
115			79	3.66	1.12	77	76	φCCC
116			69	0.11	5.71	67	66	φCCC
117			56	0.75	0.59	49	48	φCCC
118			43	0.68	1.00	46	45	φCCC
119			36	0.71	2.76	39	38	φCCN
120			28	0.08	7.63	31	31	φCCC
121			23	0.29	0.53	24	23	φCCC
122			17	0.43	2.76	17	17	φCCC
123			12	0.21	1.45	15	15	φCCC

I: IR intensity; S: Raman scattering activity; γ : stretching; β : in-plane bending; ϕ : out-of-plane bending

nature of the substituents [26, 27]. The aromatic vibrations of the title compound were observed at 3123, 3052 and 3003 cm⁻¹ in its FT-IR spectrum and at 3069 and 3034 cm⁻¹ in its FT-Raman spectrum. The remaining C-H vibrations occurred at 2925 cm⁻¹ in the FT-IR spectrum and at 2979 and 2958 cm⁻¹ in the FT-Raman spectrum.

The bands due to C-H in-plane bending vibrations are expected to be in the region of 1000–1300 cm⁻¹ [28]. The bands observed at 1182 and 973 cm⁻¹ in the FT-IR spectrum and at 1000 cm⁻¹ in the FT-Raman spectrum

were assigned to be the C-H in-plane bending vibrations of the IPAONM molecule. The theoretically scaled C-H vibrations by B3LYP/6-311G(d,p) level of theory showed good agreement with the experimentally recorded data. The C-H out-of-plane bending vibrations usually appear within the region of 900-675 cm⁻¹ [28]. The out-of-plane C-H vibrations of the title compound arose at 621 and 513 cm⁻¹ in its FT-IR spectrum and at 441 and 406 cm⁻¹ in its FT-Raman spectrum. The other C-H out-of-plane bending vibrations are within the characteristic region.



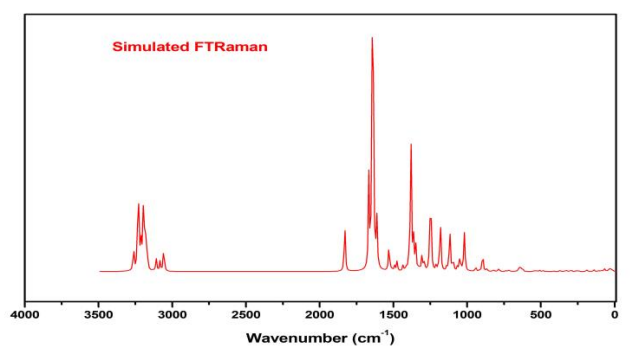


Figure 9: Simulated FT-IR and FT-Raman and spectra of the IPAONM molecule.

3.10.2 Ring Vibrations

Most of the aromatic ring modes are due to C-C bands. The ring stretching vibrations are expected within the region 1620-1390 cm⁻¹ [29]. Most of the aromatic ring modes are altered by the substitution on the ring. The C-C stretching vibrations in aromatic compounds usually form strong bands. The title compound manifested bands of different intensities at 1517, 1495, 1480, 1452, 1405, 1392, 1369 and 1304 cm⁻¹ in its FT-IR spectrum and at 1627, 1500, 1369 and 1355 cm⁻¹ in its FT-Raman spectrum and they have been assigned to be for the C-C stretching vibrations. The calculated values by B3LYP/6-311G(d,p) method are consistent with the experimental values. The theoretical ring in-plane bending and out-of-plane bending modes are also in a good agreement with experimental data. Only five infrared bands at 1104, 1078, 1025, 778 and 758

only five infrared bands at 1104, 1078, 1025, 7/8 and 758 cm⁻¹ and one Raman band at 1169 cm⁻¹ were assigned to the C–C-C in-plane bending vibrations of the IPAONM molecule. In addition, one band was assigned to the C-C-C out-of-plane bending vibration of the title molecule at 696 cm⁻¹ in its FT-IR spectrum.

3.10.3 C-N and C-O Vibrations

C-N vibrations are usually mixed with several other bands and thus it is more difficult for them to be identified in a specific region. The observed bands at 1569 and 1469 cm⁻¹ in the FT-IR spectrum of 2-formylpyridine were assigned to be due to C-N stretching [30], while they were noticed at 1580 and 1260 cm⁻¹ in ethyl pyridine [31]. In the present work, the observed bands at 1615, 1608, 1575 and 1339 cm⁻¹ in the FT-IR spectrum and at 1597 and 1500 cm⁻¹ in the FT-IR spectrum have been assigned to C-N stretching vibrations, whereas the title compound manifested CCN in-plane bending at 1031 and 929 cm⁻¹ in its FT-Raman spectrum and only one band at 929 cm⁻¹ in its FT-IR spectrum. The CCN out-of-plane bending modes were observed at 657 cm⁻¹ in the FT-IR spectrum of the IPAONM molecule and at 645 and 617 cm⁻¹ in its FT-Raman spectrum. The C-O stretching vibrations are well correlated with the experimental values at 1636 cm⁻¹ in the FT-IR spectrum and at 1285 in the FT-Raman spectrum. The calculated C-N and C-O vibration frequencies by B3LYP/6-311G(d,p) method coincide with the experimental values.

3.10.4 N-O vibrations

The N-O stretching vibration of the title compound was observed at 1751 cm⁻¹ in its FT-IR spectrum and its N-O inplane bending vibration appeared at 1240 cm⁻¹, while its N-O out-of-plane bending vibration was identified at 645 cm⁻¹ in its FT-Raman spectrum. All the theoretical values of N-O vibrations of the IPAONM molecule are in agreement with the recorded experimental data.

3.11 NMR Analysis

The calculated ¹H and ¹³C NMR chemical shift values of the IPAONM molecule are presented in Table 5 and have been compared with the experimental data. ¹H and ¹³C NMR chemical shifts are reported in ppm relative to TMS. Full geometry optimization of the IPAONM molecule was carried out at the gradient corrected density functional level of theory using the hybrid B3LYP method based on Becke's three parameters functional of DFT. Thereafter, gauge-including atomic orbital (GIAO) ¹H and ¹³C chemical shift calculations of the title compound was performed by the same method using 6-311G(d,p) basis set and integral equation formalism-polarizable continuum model (IEF-PCM)/DMSO variant.

Table 5: Theoretical and experimental 13C and 1H NMR chemical shift values (ppm) with respect to TMS in DMSO solution of the IPAONM molecule.

Atoms	Theoretical HF/6-311G(d,p)	Experimental	Atoms	Theoretical HF/6-311G(d,p)	Experimental
C1	137.3	128.5	H26	7.7	7.5
C2	142.2	131.9	H27	7.8	7.5
C3	137.9	128.5	H28	7.7	7.5
C4	139.1	128.8	H29	8.2	7.8
C5	142.8	132.8	H30	7.8	7.8
C6	138.1	128.8	H31	3.4	3.6
C7	165.7	161.4	H32	3.4	3.6
C8	36.4	30.1	H33	3.7	4.3
C9	43.5	43.0	H34	3.4	4.3
C11	126.7	119.4	H35	6.8	6.8
C12	136.5	127.3	H36	6.9	7.2
C14	148.3	137.2	H37	7.8	7.6
C17	166.4	165.1	H38	8.7	8.4
C18	145.0	133.8	H39	8.7	8.3
C20	139.4	131.2	H40	8.7	8.3
C21	134.4	123.9	H41	8.7	8.4
C22	158.1	150.4			
C23	134.6	123.9			
C24	141.9	131.2			

Atoms were numbered as illustrated in Figure 1.

Aromatic carbons gave calculated signals in the overlapped areas of the ¹³C spectrum of the title molecule with chemical shift values in the range of 134.4 to 158.1 ppm. Their corresponding experimental chemical shift values occurred in the range of 128.5-150.4 ppm. Moreover, the highest ¹³C chemical shift values were observed for C17 and C7 to be 165.1 and 161.4 ppm due to their connection to oxygen and nitrogen atoms, respectively, while the imidazole carbons C11, C12 and C14 were noticed at 119.4, 127.3 and 137.2 ppm, respectively, in which C14 is the most downfield carbon atom due to its bonding with two nitrogen atoms. One the other hand, the ethylene carbons. C8 and C9, manifested the lowest chemical shift values at 30.1 and 43.0 ppm, respectively, in the ¹³C NMR spectrum of the IPAONM molecule.

The calculated chemical shift values for the aromatic hydrogens of the title compound lie in the range of 7.7-8.7 ppm and their respective observed values occurred in the range of 7.5-8.4 ppm. The aromatic protons H38, H39, H40 and H41 are the most downfield protons due to their connection to the nitro-substituted aromatic ring, whereas the ethylene protons H31, H32, H33 and H34 appear in the range of 3.6-4.3 ppm being the most upfield protons in the ¹H NMR spectrum of the IPAONM molecule. There is a good agreement between the experimental and theoretical chemical shift values of the title compound.

4 Conclusion

A comprehensive spectroscopic profiling and vibrational analysis of the anti-Candida agent IPAONM have been performed using HF and DFT computation methods with 6-311G(d,p) basis set. The optimized geometry of the title molecule afforded only one conformer. The Mulliken charge distribution study revealed that all nitrogen atoms have negative charge except N42 and N15 is less negative than N10 and N13. The HOMO-LUMO energy gap explained the possible charge transfer inside the IPAONM molecule, which influences its biological activity. The Laplacian of charge density at the BCP1 and BCP2 of H37-H38 and H30-H32 bond critical points are 0.0069 and 0.0473 a.u., respectively. The theoretically scaled C-H vibrations by B3LYP/6-311G (d,p) method showed good agreement with the experimentally recorded data. It is believed that the results of the current exploration could support the development of new potent anti-Candida agents to be appropriate for clinical harnessing.

Supplementary information: Tables S1 and S2 as well as Scheme S1 and Figure S1 are provided as supporting information.

Acknowledgment: This work was funded by the Deanship of Scientific Research at Princess Nourah bint Abdulrahman University through the Research Group Program (Grant No. RGP-1438-0010).

Conflict of interest: Authors state no conflict of interest.

References

- [1] Ngo H.X., Garneau-Tsodikova S., Green K.D., A complex game of hide and seek: the search for new antifungals, Med. Chem. Comm., 2016, 7, 1285-1306.
- [2] Vandeputte P., Ferrari S., Coste A.T., Antifungal resistance and new strategies to control fungal infections, Int. J. Microbiol., 2012, 2012, 1-24, Article ID 713687.
- Denning D.W., Kibbler C.C., Barnes R.A., British society for medical mycology proposed standards of care for patients with invasive fungal infections, The Lancet Infect. Dis., 2003, 3, 230-240.
- [4] Kathiravan M.K., Salake A.B., Chothe A.S., Dudhe P.B., Watode R.P., Mukta M. S., Gadhwe S., The biology and chemistry of antifungal agents: a review. Bioorg. Med. Chem., 2012, 20, 5678-5698.
- [5] Holbrook S.Y., Garzan A., Dennis E.K., Shrestha S.K., Garneau-Tsodikova S., Repurposing antipsychotic drugs into antifungal agents: Synergistic combinations of azoles and bromperidol derivatives in the treatment of various fungal infections. Eur. J. Med. Chem., 2017, 139, 12-21.
- [6] Ghannoum M.A., Rice L.B., Antifungal agents: mode of action, mechanisms of resistance, and correlation of these mechanisms with bacterial resistance. Clin. Microbiol. Rev., 1999, 12, 501-517.
- [7] Sheehan D.J., Hitchcock C.A., Sibley C.M., Current and emerging azole antifungal agents. Clin. Microbiol. Rev., 1999, 12, 40-79.
- [8] Attia M.I., Ghabbour H.A., Zakaria A.S., Fun H.-K., In vitro anti-Candida activity and single crystal X-ray structure of ({(1E)-[3-(1H-imidazol-1-yl)-1-phenylpropylidene]amino}oxy) (4-nitrophenyl)methanone. Bangladesh J. Pharmacol., 2014, 9, 43-48.
- [9] Frisch M., Trucks G., Schlegel H.B., Scuseria G., Robb M., Cheeseman J., Montgomery Jr J., Vreven T., Kudin K., Burant J., Gaussian 03, revision C. 02; Gaussian, Inc. Wallingford, CT, 2004.

- [10] Arslan H., Algül Ö., Synthesis and Ab Initio/DFT Studies on 2-(4-methoxyphenyl)benzo[d]thiazole, Int. J. Mol. Sci., 2007, 8, 760-776.
- [11] Sundaraganesan N., Ilakiamani S., Saleem H., Wojciechowski P.M., Michalska D., FT-Raman and FT-IR spectra, vibrational assignments and density functional studies of 5-bromo-2nitropyridine, Spectrochim. Acta A Mol. Biomol. Spectrosc., 2005, 61, 2995-3001.
- [12] Jamróz M.H., Vibrational energy distribution analysis (VEDA): scopes and limitations. Spectrochim. Acta A Mol. Biomol. Spectrosc., 2013, 114, 220-230.
- Dennington R., Keith T., Millam J., Eppinnett K., Hovell W., Gilliland R.G., Version 3.09, Semichem. Inc., Shawnee Mission,
- [14] Fleming I., Frontier orbitals and organic chemical reactions, Wiley, 1977.
- [15] Kosar B., Albayrak C., Spectroscopic investigations and quantum chemical computational study of (E)-4-methoxy-2-[(ptolylimino)methyl]phenol, Spectrochim. Acta A Mol. Biomol. Spectrosc., 2011, 78, 160-167.
- [16] Luque F., Orozco M., Bhadane P., Gadre S., SCRF calculation of the effect of water on the topology of the molecular electrostatic potential. J. Phys. Chem., 1993, 97, 9380-9384.
- [17] Murray J.S., Sen K., Molecular electrostatic potentials: concepts and applications, Elsevier, 1996, Vol. 3.
- [18] Alkorta I., Perez J.J., Molecular polarization potential maps of the nucleic acid bases, Int. J. Quantum Chem., 1996, 57, 123-135.
- [19] Silverstein R.M., Webster F.X., Kiemle D.J., Bryce D.L., Spectrometric identification of organic compounds, John Wiley & Sons, USA, 2014.
- [20] Gorelsky S., SWizard Program Revision 4.5, University of Ottawa, Ottawa, Canada, 2010.
- [21] Bader R.F.W., Atoms in molecules, A quantum theory, Clarendon: Oxford, UK, 1990.
- [22] Biegler-Konig F., Schonbohm J., Bayles D., Software news and updates-AIM2000-A program to analyze and visualize atoms in molecules. John Wiley & Sons Inc. 605 Third Ave, New York, NY, USA, 2001, 22, 545-559.
- [23] Carroll M.T., Bader R.F., An analysis of the hydrogen bond in BASE-HF complexes using the theory of atoms in molecules, Mol. Phys., 1988, 65, 695-722.
- [24] Koch U., Popelier P., Characterization of CHO hydrogen bonds on the basis of the charge density, J. Phys. Chem., 1995, 99, 9747-9754.
- [25] Carroll M.T., Chang C., Bader R.F., Prediction of the structures of hydrogen-bonded complexes using the Laplacian of the charge density, Mol. Phys., 1988, 63, 387-405.
- [26] Socrates G., Infrared and Raman characteristic group frequencies: tables and charts, John Wiley & Sons, USA, 2004.
- [27] Colthup N., Introduction to infrared and Raman spectroscopy, Elsevier, 2012.
- [28] Jamróz M.H., Dobrowolski J.C., Brzozowski R., Vibrational modes of 2, 6-, 2, 7-, and 2, 3-diisopropylnaphthalene. A DFT study, J. Mol. Struct., 2006, 787, 172-183.
- [29] Madhavan V., Varghese H.T., Mathew S., Vinsova J., Panicker C.Y., FT-IR, FT-Raman and DFT calculations of 4-chloro-2-(3,4dichlorophenylcarbamoyl) phenyl acetate, Spectrochim. Acta A Mol. Biomol. Spectrosc., 2009, 72, 547-553.

DE GRUYTER

- [30] Umar Y., Density functional theory calculations of the internal rotations and vibrational spectra of 2-, 3-and 4-formyl pyridine., Spectrochim. Acta A Mol. Biomol. Spectrosc., 2009, 71, 1907-1913.
- [31] Shakila G., Periandy S., Ramalingam S., Molecular structure and vibrational analysis of 3-Ethylpyridine using ab initio HF and density functional theory (B3LYP) calculations, Spectrochim. Acta A Mol. Biomol. Spectrosc., 2011, 78, 732-739.

Supplemental Material: The online version of this article offers supplementary material (https://doi.org//10.1515/chem-2018-0005).